Analysis of Molecular Activated Recombination in Detached Divertor Plasmas*)

Yuka TSUBOTANI, Ryoko TATSUMI, Kazuo HOSHINO and Akiyoshi HATAYAMA

Graduate School of Science and Technology, Keio University, Yokohama 223-8522, Japan

(Received 28 September 2018 / Accepted 29 January 2019)

Molecular activated recombination (MAR) has been received attention as one of the most important processes to realize the detached state, specifically in the linear plasma device, GAMMA10/PDX. The impact of ELMs on the MAR reaction and the resultant detached state, however, have not fully been understood. We have developed a zero-dimensional model of atomic-molecular processes which takes into account MAR by separate treatment of vibrational excited states of H_2 molecules, and the high energy tail of the electron energy distribution function (EEDF) during the ELM heat pulse. The results show that the rate of MAR increases during ELMs due to an increase in excited molecules.

Keywords: MAR, ELM, detachment state, GAMMA10/PDX, 0D model

DOI: 10.1585/pfr.14.2403108

1. Introduction

It is important to understand the dynamic behavior of detachment, especially the response to the heat pulse during Edge Localized Modes (ELMs). To analyze it, we have focused on the following two points.

The first point is non-equilibrium electron energy distribution function (EEDF) during ELMs. In the high confinement H-mode plasma, high temperature and density heat pulse flows into the divertor plate due to ELMs. High energy particles due to ELMs may collapse the detached plasma that is realized under the low temperature condition. It has been clarified numerically that the energy distribution of plasma during the ELM deviates from thermodynamic equilibrium with Maxwellian distribution [1]. Therefore, to analyze the detachment during ELMs, a dynamic model including a non-equilibrium feature of the EEDF is necessary.

The second point is the effect of molecular activated recombination (MAR) on the detached state [2, 3]. The volume recombination, which is important process for the detached state, is classified into two types, 1) ion electron recombination (IER) and 2) MAR which occurs via vibrational excited molecules. There are two types of IER: radiative recombination (Eq. (1)) and three body recombination (Eq. (2)).

$$e + H^+ \rightarrow H + h\upsilon, \tag{1}$$

$$e + e + H^+ \rightarrow e + H. \tag{2}$$

As for MAR, two paths are taken into account in this study. One is IC-MAR starting with ion conversion (IC) and causing dissociative recombination (DR).

$$\mathrm{IC:}\ H_2(\upsilon) + H^+ \rightarrow H_2^+ + H(1s), \tag{3}$$

$$\mathrm{DR:}\ H_2^+ + e \rightarrow H(1s) + H(p), \tag{4}$$

where υ is the vibrational excitation level, and p is the principal quantum number of H. The other path is DA-MAR starting with dissociative attachment (DA) and leading to mutual neutralization (MN).

$$\mathrm{DA:}\ H_2(\upsilon) + e \rightarrow H^- + H(1s), \tag{5}$$

$$\mathrm{MN:}\ H^- + H^+ \rightarrow H(1s) + H(p = 2, 3). \tag{6}$$

From Ref. [2], the MAR rate is higher than IER, which suggests MAR can significantly contribute to detachment. Recently, it has been reported that MAR greatly contributes to detachment in the linear plasma device, GAMMA10/PDX [4]. In tokamak devices, however, MAR has not been clearly observed. It still remains an issue to analyze what conditions make MAR dominant.

In order to analyze (1) the role of MAR for detachment and (2) dynamic response to detachment by ELMs, we are developing a simple zero-dimensional (0D) model of atomic-molecular processes which takes into account non-equilibrium features of the EEDF and the effect of MAR.

2. Model

To analyze dynamic behavior of detachment, a 0D model of atomic molecular processes has been developed. Some geometry parameters are chosen in reference to GAMMA10/PDX, in which MAR has been observed.

2.1 0D model

The 0D model is a so-called rate equation which is derived from the transport equation by the volume integral.

author's e-mail: tsubotani@ppl.appi.keio.ac.jp

*) This article is based on the presentation at the 12th International Conference on Open Magnetic Systems for Plasma Confinement (OS2018).

Therefore, the model does not consider the spatial distribution. The basic equation of this 0D model is as follows:

$$\frac{\mathrm{d}n_s}{\mathrm{d}t} = \sum_{j,k} R_{\mathrm{gain}} n_j n_k - \sum_{l,m} R_{\mathrm{loss}} n_l n_m - \frac{n_s}{\tau_{\mathrm{trans}}} + S_{\mathrm{gain}}, \tag{7}$$

where n is the density of particle species, s = electron, H^+, H^-, H_2^+, H (principal quantum number $p = 1{\sim}35$) and H_2 (vibrational excited level $v = 0{\sim}14$). The symbols j, k, l and m indicate combinations of the particle species which produce/extinguish the particle species s by the reactions taken into account in the 0D model (See Table 1). The symbols R_{gain}, R_{loss}, τ_{trans} and S_{gain} are the rate coefficient of production reaction, the rate coefficient of loss reaction, confinement time, and the particle source term, respectively. As for the particle source term S_{gain}, it represents H_2 gas puffing constant ($S_{\mathrm{H}_2} = 2 \times 10^{21}\,\mathrm{m}^{-3}\mathrm{s}^{-1}$) in the equation for H_2, while it describes the volume source due to plasma inflow from the upstream to the divertor region in the equations for the electron and H^+. The time evolution of each particle density is calculated by the rate equation, Eq. (7), by calculating the rate coefficients R as

$$R = \int \sigma(E) v(E) f(E) \mathrm{d}E, \tag{8}$$

where $\sigma(E)$, $v(E)$ and $f(E)$ are the reaction cross section, relative velocity and EEDF, respectively. The EEDF used in this study will be explained later. The confinement time τ_{trans} for the plasmas (H^+, H^- and H_2^+) are calculated by using ion sound velocity C_{s} as follows:

$$\tau_{\mathrm{trans}} = 100 \frac{L}{C_{\mathrm{s}}}, \tag{9}$$

$$C_{\mathrm{s}} = \sqrt{\frac{k_{\mathrm{B}} T_{\mathrm{e}}}{m_{\mathrm{s}}}}, \tag{10}$$

Table 1 Reactions included in the 0D model.

The name of the reaction		Equation	Rate coefficient
Vibrational Excitation / De-excitation	eV	$\mathrm{e} + \mathrm{H}_2(\mathrm{X}^1\Sigma_g^+; v) \to \mathrm{H}_2^- \to \mathrm{e} + \mathrm{H}_2(\mathrm{X}^1\Sigma_g^+; v')$	$R_{\mathrm{eV}(v\to v')}$
	EV	$\mathrm{e} + \mathrm{H}_2(\mathrm{X}^1\Sigma_g^+; v) \to \mathrm{e} + \mathrm{H}_2(\mathrm{B}^1\Sigma_u^+, \mathrm{C}^1\Pi_u) \to \mathrm{e} + \mathrm{H}_2(\mathrm{X}^1\Sigma_g^+; v')$	$R_{\mathrm{EV}(v\to v')}$
IC		$\mathrm{H}_2(v) + \mathrm{H}^+ \to \mathrm{H}_2^+ + \mathrm{H}(1s)$	$R_{\mathrm{IC}}(v)$
DA		$\mathrm{H}_2(v) + \mathrm{e} \to \mathrm{H}^- + \mathrm{H}(1s)$	$R_{\mathrm{DA}}(v)$
DR		$\mathrm{H}_2^+ + \mathrm{e} \to \mathrm{H}(1s) + \mathrm{H}(n)$	R_{DR}
MN		$\mathrm{H}^- + \mathrm{H}^+ \to \mathrm{H}(n = 2, 3) + \mathrm{H}(1s)$	R_{MN}
H_2 Dissociation		$\mathrm{H}_2(v) + \mathrm{e} \to \mathrm{H}_2(\mathrm{b}^3\Sigma_u^+) + \mathrm{e} \to \mathrm{e} + \mathrm{H}(1s) + \mathrm{H}(1s)$	$R_{\mathrm{FC}}(v)$
H^- loss		$\mathrm{H}^- + \mathrm{e} \to \mathrm{H}(1s) + \mathrm{e} + \mathrm{e}$	R_{ED}
H_2^+ Dissociation		$\mathrm{H}_2^+ + \mathrm{e} \to \mathrm{H}^+ + \mathrm{H}(1s) + \mathrm{e}$	R_{DE}
H_2 Ionization		$\mathrm{H}_2(v) + \mathrm{e} \to \mathrm{H}_2^+ + 2\mathrm{e}$	$R_{\mathrm{MI}}(v)$
Dissociative Ionization		$\mathrm{H}_2(v) + \mathrm{e} \to \mathrm{H}_2^+(\mathrm{B}^2\Sigma_u^+) + 2\mathrm{e} \to \mathrm{H}^+ + \mathrm{H}(1s) + 2\mathrm{e}$ $\mathrm{H}_2(v) + \mathrm{e} \to \mathrm{H}_2^+(\mathrm{X}^2\Sigma_g^+) + 2\mathrm{e} \to \mathrm{H}^+ + \mathrm{H}(1s) + 2\mathrm{e}$	$R_{\mathrm{DI}}(v)$
H Excitation		$\mathrm{H}(p) + \mathrm{e} \to \mathrm{H}(q) + \mathrm{e} \quad (p < q)$	$C(p,q)$
H De-excitation		$\mathrm{H}(p) + \mathrm{e} \to \mathrm{H}(q) + \mathrm{e} \quad (p > q)$	$F(p,q)$
H Ionization		$\mathrm{H}(p) + \mathrm{e} \to \mathrm{H}^+ + 2\mathrm{e}$	$S(p)$
Three-Body Recombination		$\mathrm{H}^+ + \mathrm{e} + \mathrm{e} \to \mathrm{H}(p) + \mathrm{e}$	$R_{\mathrm{TBR}}(p)$
Radiative Recombination		$\mathrm{H}^+ + \mathrm{e} \to \mathrm{H}(p) + h\nu$	$R_{\mathrm{RR}}(p)$
Spontaneous Emission		$\mathrm{H}(q) \to \mathrm{H}(p) + h\nu$	$A(p,q)$

where m_{s} is the mass of each plasma constituent and T_{e} is the electron temperature. For C_{s} and the resultant τ_{trans} of the electron, the H^+ ion mass is used instead of the electron mass, because electrons escape from the system as a resultant of the balance with ions due to the sheath. Here, the factor 100 in Eq. (9) has been added to focus on the time scale due to atomic molecular processes rather than the transport time scale in this initial calculation. In the future, we will look into the effects of the transport loss by taking confinement time as a parameter. The system length L in Eq. (9) was chosen as $L = 0.7\,\mathrm{m}$ in the present model, in reference to the length of the D-module of GAMMA10/PDX. The confinement time τ_{trans} for the neutral particles (H (p: 1∼35) and H_2 (v: 0∼14)) are estimated as a simple diffusive characteristic time.

2.2 Method of the ELM simulation

To simulate ELMs, electrons are divided into low energy components (electron temperature is T_{e1}, density is n_{e1}) and high energy components by ELMs (electron temperature is T_{e2}, density is n_{e2}). As shown in Fig. 1, an ELM is simulated by inputting a high-energy electron particle source of 100 eV after calculating each rate equation up to the steady state in a detached state with an electron temperature of 1 eV. The inflow of 1 eV electrons from the upstream (the volume source) is $S_{\mathrm{e}}(1\,\mathrm{eV}) = 4.6 \times 10^{20}\,\mathrm{m}^{-3}\mathrm{s}^{-1}$, and the inflow of 100 eV electrons by the ELM is $S_{\mathrm{e}}(100\,\mathrm{eV}) = 4.6 \times 10^{19}\,\mathrm{m}^{-3}\mathrm{s}^{-1}$. The ELM duration is set to be $\Delta t_{\mathrm{ELM}} = 200\,\mu\mathrm{s}$. The ELM pulse starts at 1.0×10^{-4} s and ends at 3.0×10^{-4} s.

The EEDF during the ELM is assumed as a double Maxwellian distribution as follows

$$f(E) = \alpha f_{\mathrm{M}}(T_{\mathrm{e1}}) + (1 - \alpha) f_{\mathrm{M}}(T_{\mathrm{e2}}), \tag{11}$$

$$\alpha = \frac{n_{\mathrm{e1}}}{n_{\mathrm{e1}} + n_{\mathrm{e2}}}. \tag{12}$$

In Eq. (11), $f_{\mathrm{M}}(T_{\mathrm{e}})$ is Maxwellian distribution as follows:

$$f_{\mathrm{M}}(T_{\mathrm{e}}) = \frac{2}{\sqrt{\pi}} \frac{\sqrt{E}}{(k_{\mathrm{B}} T_{\mathrm{e}})^{3/2}} \exp\left(\frac{-E}{k_{\mathrm{B}} T_{\mathrm{e}}}\right), \tag{13}$$

$$T_{\mathrm{e}} = T_{\mathrm{e1}}, T_{\mathrm{e2}},$$

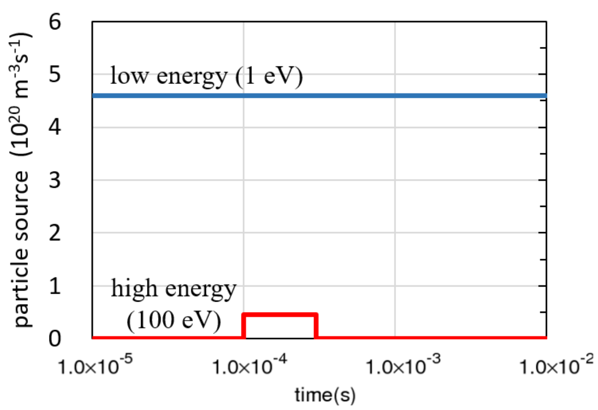

Fig. 1 Electron particle source in the simulation.

where k_B, T_e and E are the Boltzmann constant, electron temperature and energy, respectively. The EEDF calculated by Eq. (11) is substituted into the calculation of the rate coefficient every time step, in order to take into account its time development.

The low energy electron temperature is fixed at T_{e1} = 1 eV. On the other hand, the high energy electron temperature T_{e2} has been calculated by a 0D simple energy balance equation as follows:

$$\frac{d}{dt}\left(\frac{3}{2}n_{e2}T_{e2}\right) = -E_{ion} \times n_{e2}n_H R_{ioz} + \frac{3}{2} \times E_{ELM} \times S_{e2} - \frac{\frac{3}{2}n_{e2}T_{e2}}{\tau_{trans}}, \tag{14}$$

where E_{ion} and E_{ELM} are the energy lost by H ionization E_{ion} = 13.6 eV and gained from the ELM E_{ELM} = 100 eV, respectively. The third term on the RHS of Eq. (14) represents the energy loss due to transport, and τ_{trans} is calculated by Eq. (9).

3. Results and Discussion

The time evolution of each particle density is shown in Fig. 2. The low energy electron density and neutral particle density in the ground state are not affected greatly by the ELM pulse. The high energy electron density and H^+ density increase during the ELM. After the ELM, high energy electron density decreases and returns to the detached state before the ELM.

Figure 3 shows the calculated result of high energy electron temperature T_{e2}. Immediately after the start of the ELM, electrons of 100 eV by the ELM pulse are rapidly cooled and the temperature drops due to the ionization. As a result, the high energy electron temperature T_{e2} during the ELM is about 2 eV to 3 eV. After the ELM, the temperature further drops to 1 eV.

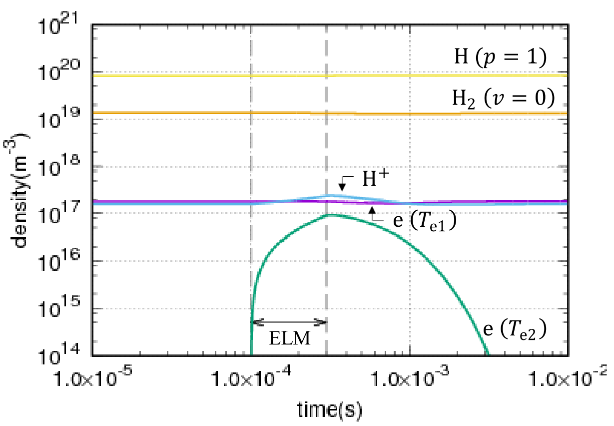

Fig. 2 The time evolution of density of low energy electron, high energy electron, H^+, ground state of H_2 molecule and ground state of H atom.

The rates of recombination (MAR and IER) and H ionization (IOZ) are calculated to evaluate the contribution of MAR, IER and IOZ to detachment as follows,

$$\mathrm{MAR} = R_{DR}n_{H_2^+}n_e + R_{MN}(p)n_{H^+}n_{H^-}, \tag{15}$$

$$\mathrm{IER} = \sum_p (R_{TBR}(p)n_{H^+}n_e^2 + R_{RR}(p)n_{H^+}n_e), \tag{16}$$

$$\mathrm{IOZ} = \sum_p S(p)n_H(p)n_e, \tag{17}$$

where MAR, IER and IOZ show MAR rate, IER rate and H ionization rate. Figure 4 shows the calculation results of MAR, IER and H ionization rate. It can be seen that the ionization rate rapidly increases just after the start of the ELM pulse due to the heat pulse of high energy electrons. Also, the recombination rate of IER increases during the ELM. This is due to the increase in plasma density by H ionization just after the start of the ELM pulse. Since the rate of three body recombination is proportional to the square of the plasma density, the plasma density greatly contributes to the IER rate.

It can be seen from Fig. 4 that the MAR rate also increases during the ELM. This tendency can be explained

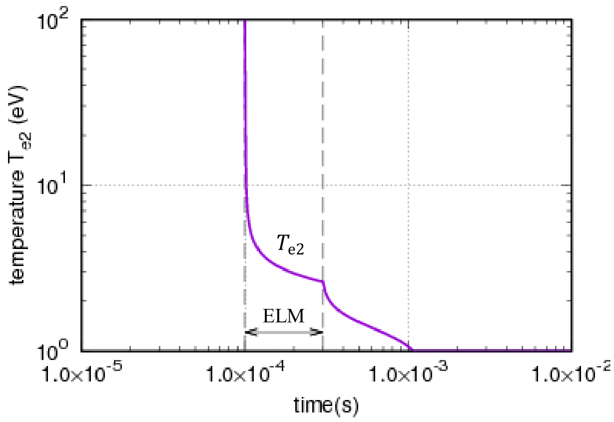

Fig. 3 The calculation result of high energy electron temperature T_{e2}.

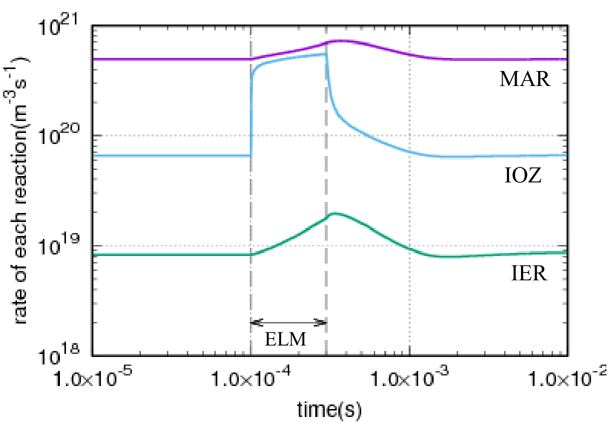

Fig. 4 Rate of MAR, IER and H ionization.

from the rate coefficient and the density of vibrational excited molecules. Figure 5 shows the effective rate coefficients of IC-MAR, DA-MAR and H ionization as a function of electron temperature T_e. Here, the electron density of 1×10^{17} m^{-3} is assumed to estimate the effective rate coefficients. It is shown that the rate coefficient of IC-MAR is larger than that of the DA-MAR in the electron temperature range of 1 eV < T_e < 100 eV. At low energy electron temperature T_{e1} = 1 eV before the ELM and high energy electron temperature T_{e2} = 2~3 eV during the ELM, the ionization rate coefficient changes greatly, but the IC-MAR rate coefficient does not change so much.

Figure 6 shows the time evolution of the density of each level of vibrational excited molecules. The density of high excited level molecules increases during the ELM

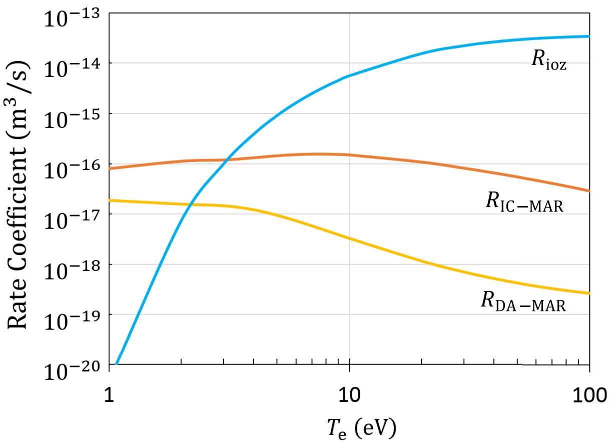

Fig. 5 Rate coefficients of IC-MAR, DA-MAR and H ionization as a function of electron temperature T_e. Vibrational excited states of 0~14 are considered for the MAR rate, while only ground state is considered for the ionization rate.

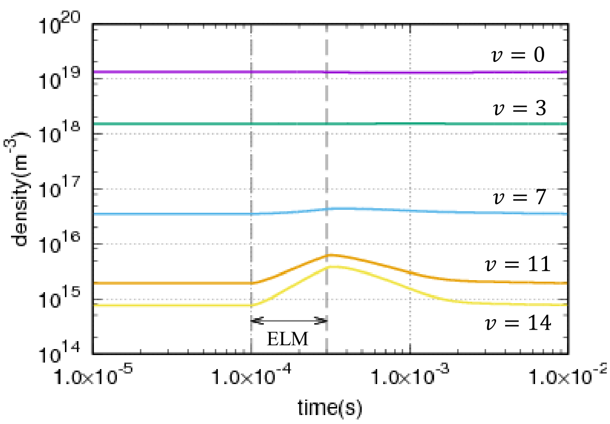

Fig. 6 The time evolution of each level of vibrational excited molecules.

due to the increase of high energy electrons. Such high excited level molecules contribute to enhancement of the MAR reaction.

As seen above, with increasing T_e from 1 eV to 4 eV, the MAR rate coefficient does not change and the density of high excited level molecules increase. Therefore, the total MAR reaction rate increases.

Now we compare the rate of recombination (the sum of MAR and IER) and that of H ionization (IOZ) to understand which process is dominant in the detached state. From Fig. 4, because of the MAR rate, the recombination rate is larger than the ionization rate. Therefore, the plasma loss rate is still more dominant than the plasma production rate even during the ELM under the current calculation condition, which suggests MAR is effective to maintain the detachment. As the MAR rate increases during the ELM, MAR can suppress the collapse of detachment due to ionization even during the ELM.

4. Summary and Future Plan

In order to investigate the impact of the ELM on the MAR reaction and the resultant detached state, we have developed a 0D model of atomic-molecular processes. By using the model, the following result has been obtained. MAR rate increases due to the increase in high excited level molecules during the ELM pulse and its rate coefficient does not change so much even during the ELM. This result suggests that MAR can suppress the collapse of the detached state due to ionization even during the ELM.

In the 0D model, however, effects of the spatial profiles and transport are neglected. Especially in this calculation condition, the confinement time is set to be long to reduce the effect of transport. In addition, the high energy electron temperature T_{e2} is calculated by a simple 0D energy equation as well as a simple model that has been used to evaluate the EEDF during the ELM heat pulse. In order to obtain a deeper and more precise understanding of the dynamic behavior of detachment, it is necessary to improve these points in the model.

For the improvement of the model, we are developing a 1D/2D particle in cell (PIC) model and a 3D neutral particle transport model in order to evaluate more precisely the plasma confinement time and also to calculate the EEDF during the ELM. In the future, the 3D neutral particle transport model and the 1D/2D PIC model will be integrated and the integrated code will be applied to the dynamic analysis of detachment during ELM pulses.

[1] T. Shibata *et al.*, J. Nucl. Mater. **415**, 873 (2011).
[2] A.Y. Pigarov *et al.*, Phys. Lett. A **222**, 251 (1996).
[3] S.I. Krasheninnikov *et al.*, Phys. Scr. **T96**, 7 (2002).
[4] M. Sakamoto *et al.*, Nucl. Mater. Energy **12**, 1004 (2017).